◆ Human Brain Mapping 35:4140–4154 (2014) ◆

Pupil Diameter Covaries With BOLD Activity in Human Locus Coeruleus

Peter R. Murphy,* Redmond G. O'Connell, Michael O'Sullivan, Ian H. Robertson, and Joshua H. Balsters

Trinity College Institute of Neuroscience and School of Psychology, Trinity College Dublin, Dublin 2, Ireland

Abstract: The locus coeruleus-noradrenergic (LC–NA) neuromodulatory system has been implicated in a broad array of cognitive processes, yet scope for investigating this system's function in humans is currently limited by an absence of reliable non-invasive measures of LC activity. Although pupil diameter has been employed as a proxy measure of LC activity in numerous studies, empirical evidence for a relationship between the two is lacking. In the present study, we sought to rigorously probe the relationship between pupil diameter and BOLD activity localized to the human LC. Simultaneous pupillometry and fMRI revealed a relationship between continuous pupil diameter and BOLD activity in a dorsal pontine cluster overlapping with the LC, as localized via neuromelanin-sensitive structural imaging and an LC atlas. This relationship was present both at rest and during performance of a two-stimulus oddball task, with and without spatial smoothing of the fMRI data, and survived retrospective image correction for physiological noise. Furthermore, the spatial extent of this pupil/LC relationship guided a volume-of-interest analysis in which we provide the first demonstration in humans of a fundamental characteristic of animal LC activity: phasic modulation by oddball stimulus relevance. Taken together, these findings highlight the potential for utilizing pupil diameter to achieve a more comprehensive understanding of the role of the LC–NA system in human cognition. *Hum Brain Mapp 35:4140–4154, 2014.*

Key words: pupillometry; fMRI; noradrenaline; norepinephrine; resting state; oddball; attention

INTRODUCTION

The locus coeruleus (LC) is a small nucleus in the dorsal pons that exerts powerful effects on neural processing via secretion of the neuromodulator noradrenaline [NA; Berridge and Waterhouse, 2003; Sara, 2009]. Inspired predominantly by studies of single-cell LC activity in animals [e.g., Aston-Jones et al., 1994; Bouret and Sara, 2004; Clayton et al., 2004; Rajkowski et al., 1994, 2004], a number of sophisticated theoretical models have been devised that implicate this system in core neuro-cognitive processes like the regulation of task engagement [Aston-Jones and Cohen, 2005; Bouret and Sara, 2005; Sara and Bouret, 2012; Usher et al., 1999] and learning [Dayan and Yu, 2006; Verguts and Notebaert, 2009; Yu and Dayan, 2005]. However, current scope for testing theory-driven hypotheses of LC-NA function in humans is greatly constrained by a lack of

Additional Supporting Information may be found in the online version of this article.

Contract grant sponsors: Irish Research Council for Science, Engineering and Technology (IRCSET); "Embark Initiative" Grant; IRCSET Post-doctoral Fellowship; HEA PRTLI Cycle 3 Program of the EU Structural Funds; Irish Government's National Development Plan 2002–2006.

*Correspondence to: Peter Murphy, Trinity College Institute of Neuroscience, Lloyd Building, Trinity College Dublin, Dublin 2, Ireland. E-mail: murphyp7@tcd.ie

Received for publication 8 July 2013; Revised 3 December 2013; Accepted 6 January 2014.

DOI 10.1002/hbm.22466

Published online 7 February 2014 in Wiley Online Library (wileyonlinelibrary.com).

noninvasive measures capable of indexing changes in this system's activity. As a consequence, impressive theoretical developments have not been paralleled by commensurate empirical advances in our understanding of human LC-NA function.

Pupil diameter has recently emerged as a promising candidate proxy measure for LC activity, and is being increasingly employed for this purpose [Einhauser et al., 2008; Gilzenrat et al., 2010; Jepma and Nieuwenhuis, 2011; Kuipers and Thierry, 2011; Murphy et al., 2011; Nassar et al., 2012; Preuschoff et al., 2011; Smallwood et al., 2011, 2012]. Indeed, recent studies have reported that pupil diameter tracks changes in the exploration-exploitation trade-off [Gilzenrat et al., 2010; Jepma and Nieuwenhuis, 2011] and the uncertainty associated with incoming task-relevant information [Nassar et al., 2012; Preuschoff et al., 2011] in ways that are generally consistent with prominent accounts of LC-NA function [Aston-Jones and Cohen, 2005; Yu and Dayan, 2005]. However, the promise of these observations is tempered by the fact that, aside from indirect pharmacological manipulation [Hou et al., 2005] and an unpublished primate single-unit recording study [Rajkowski et al. 1993], no evidence actually exists to support an anatomical or functional connection between LC neurons and the pupil.

In this study, we use simultaneous pupillometry and blood-oxygen-level-dependent (BOLD) functional magnetic resonance imaging (fMRI) to comprehensively interrogate the relationship between fluctuations in pupil diameter and human LC activity, both at rest and during performance of the classic two-stimulus oddball paradigm. Previous studies employing conventional fMRI have demonstrated task-related activity in the vicinity of the LC across a range of settings [e.g., Berman et al., 2008; Kahnt and Tobler, 2013; Krebs et al., 2013; Liddell et al., 2005; Minzenberg et al., 2008; Mohanty et al., 2008; Raizada and Poldrack, 2007; Schilbach et al., 2011; Schmidt et al., 2009; Sterpenich et al., 2006; van Marle et al., 2010; Vandewalle et al., 2007]. However, the reliability of these findings has been questioned due to several technical difficulties inherent in brainstem imaging [Astafiev et al., 2010]. Specifically, the majority of previous LC-fMRI studies have not attempted to precisely localize the LC, have employed image processing techniques that are ill-suited to the analysis of comparatively small subcortical brain regions, and have failed to control for physiologically driven noise in the BOLD signal to which braintstem nuclei like the LC are particularly sensitive [see Payzan-LeNestour et al., 2013 for a recent exception].

To address the above methodological issues, we adopt an approach that utilizes a combination of precise structural localization via neuromelanin-sensitive imaging [Shibata et al., 2006] and a previously published LC atlas [Keren et al., 2009], retrospective statistical control for sources of physiological noise [Glover et al., 2000], and fMRI analyses with and without spatial smoothing. This approach allowed us to explore the relationship between pupil diameter and LC BOLD activity with unprecedented methodological rigour.

MATERIALS AND METHODS

Participants

Fourteen healthy, right-handed individuals [age range: 21–48 years; mean age: 29 years (± 7.7); 8 male] participated in the study after providing written informed consent. All protocols were approved by the Trinity College Dublin School of Psychology Ethics Committee and carried out in accordance with the Declaration of Helsinki. Four additional participants were tested but excluded from all analyses after inspection revealed excessive artefacts in their pupil data (see below).

Behavioral Protocols

All participants underwent a resting-state scan first and performed a visual oddball task second. During rest, participants were instructed to relax, think of nothing in particular and maintain fixation for 8 min at a centrally presented crosshair (subtending 0.65° of the visual angle). The oddball task is a simple attentional paradigm with well-characterized effects on pupil diameter in humans [Gilzenrat et al., 2010; Murphy et al., 2011] and LC activity in non-human primates [Aston-Jones et al., 1994; Rajkowski et al., 1994, 2004]. Participants were instructed to maintain fixation at a centrally presented cross (purple against a dark-grey background approximately matched for luminance, subtending 0.65° of the visual angle) and monitored a series of sequentially presented standard and target stimuli (purple circles with diameters subtending 3.2° and 1.6° of the visual angle, respectively). Target detection was indicated via speeded, right-handed thumb-press using a two-button MRI-compatible response box. All stimuli were presented for 75 ms, and targets were pseudorandomly interspersed throughout the task such that they constituted 20% of the total number of trials. The interstimulus interval varied pseudorandomly between 2.5 and 3.5s, with a total of 79 targets and 317 standards over the entire task. The stimulus array was designed to ensure a minimum inter-target interval of 10 s. The total duration of the oddball task was ~20 min, with no breaks. All stimuli were realized using the Cogent 2000 toolbox for Matlab, and presented through the eye-tracker apparatus (see below).

Magnetic Resonance Imaging and Preprocessing

Participants lay supine in an MRI scanner (Philips 3T Achieva; 8-channel head coil). Initially, high-resolution images of the LC were acquired using T1 turbo-spin-echo (TSE) structural scans [Shibata et al., 2006] with scan resolution of 256 mm × 204 mm, in-plane resolution of 0.35 mm × 0.35 mm, field of view (FOV) = 180 mm × 23 mm × 180 mm, echo time (TE) = 10 ms, repetition time

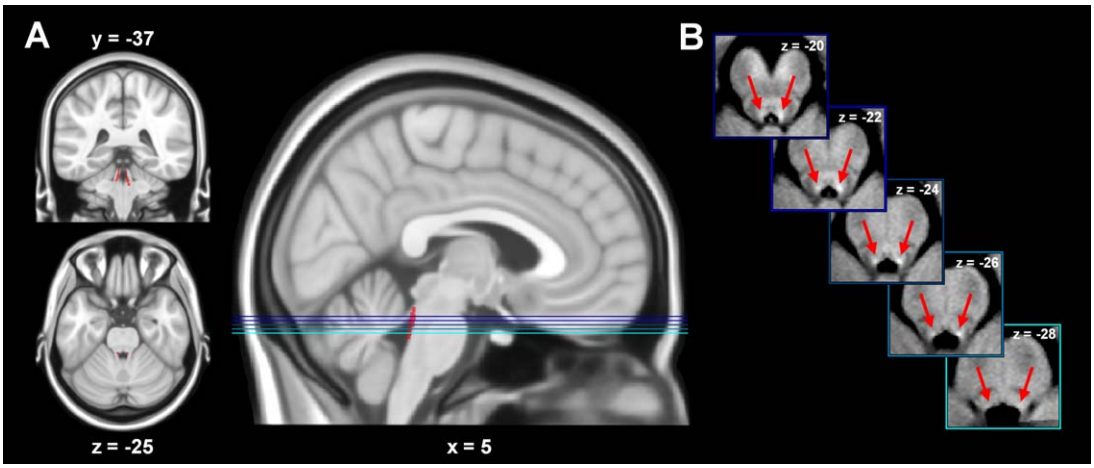

Figure 1.

Anatomical localization of the LC. **A**, Spatial extent of the binary LC atlas [Keren et al., 2009; displayed in red] overlayed onto a canonical whole brain image. **B**, Multiple axial slices (highlighted in sagittal image in A), of the group-mean high-resolution T1 TSE structural image. White arrows highlight position of LC nuclei. [Color figure can be viewed in the online issue, which is available at wileyonlinelibrary.com.]

(TR) = 500 ms, and flip angle = 90°. Each scan consisted of fourteen 1.6-mm-thick axial slices with no gaps, and took ~8 min. Each participant's LC acquisition volume was aligned via the mid-sagittal slice of a localizer scan. All participants then underwent two separate echo-planar-imaging (EPI) scanning runs for resting-state and oddball fMRI data acquisition, containing 240 and 613 volumes and lasting 8 and 20.4 min, respectively. For both runs, the FOV covered the whole brain, 224 mm × 224 mm (64 × 64 voxels), and 39 axial slices were acquired with a voxel size of 3.5 mm× 3.5 mm × 3.5 mm (0.3 mm slice gap), TE = 30 ms, TR = 2 s, flip angle = 90°. Lastly, a high-resolution T1-weighted anatomic MPRAGE image [FOV = 230 mm, thickness = 0.9 mm, voxel size = 0.9 mm× 0.9 mm× 0.9 mm] was acquired for the whole brain.

Preprocessing of MRI data was performed using SPM 8 (www.fil.ion.ucl.ac.uk/spm). EPI data quality tests were initially conducted by assessing the mean and standard deviation of signal time courses and visual inspection of mean and variance images. All EPI data collected passed these tests. Images were realigned to correct for motion artefacts, slice-time corrected to the middle temporal slice, and normalized to the international consortium for brain mapping (ICBM) EPI template using the unified segmentation approach [Ashburner and Friston, 2005]. Data were then resliced to a voxel resolution of 2-mm isotropic. For all analyses with spatially smoothed data (see Results section), a Gaussian kernel of 6-mm full width at half maximum (FWHM) was applied to all EPI images.

All T1 TSE images were co-registered to their corresponding whole brain structural images and warped into standard Montreal neurological institute (MNI) space using the same normalization parameters applied to the EPI data. Once all images were in the same space, we created a group-average T1 TSE image (Fig. 1) that could later be used for precise anatomical localization of functional effects in the dorso-rostral brainstem.

Pupillometry

Pupil diameter was recorded continuously from the left eye at rest and during task using an iView X MRI-SV eye-tracker (SMI, Needham, MA) at a sampling rate of 60 Hz. Pupillometric data were acquired via fiber-optic goggles with an integrated infrared camera. The goggles were affixed to the MRI scanner head coil and simultaneously used for the presentation of all stimuli.

Noisy and unreliable pupil data represented a crucial potential source of error when attempting to model the pupil/LC relationship. Pupillometric data were therefore subjected to the following stringent pre-processing steps offline: (1) A participant was excluded from all analyses if they provided a raw pupil dataset in which 25% of samples either contained amplitudes of <1.5 mm or represented a change in amplitude of >0.075 mm relative to the directly preceding sample ($n = 4$). (2) For the remaining participants ($n = 14$), eye-blinks and other artefacts were removed using a custom linear interpolation algorithm that restricted interpolation to periods of data loss shorter than 1 second. (3) Data were segmented into epochs from 0 to +2 s relative to the acquisition onset of each fMRI volume. Within each epoch, amplitude (any sample < 1.5 mm) and variability (any sample ± 3 s.d. outside the epoch mean) thresholds were applied to identify artefactual samples which survived Step 2. An average pupil diameter measure was then calculated for the corresponding

volume by taking the mean across the remaining non-artifactual samples in that epoch (mean proportion: rest = 98.4%, s.d. = 2.11%; task = 95.58% s.d. = 6.11%). This step is equivalent to time-locking the continuous pupil data to the onset of fMRI data acquisition and downsampling to the temporal resolution of the EPI sequence (0.5 Hz) using only clean data samples. (4) Mean pupil diameter for any epoch characterized by >40% artifactual samples (mean proportion of epochs: rest = 1.07%, s.d. = 2.16%; task = 3.98%, s.d. = 6.78%) was replaced via linear interpolation across adjacent clean epochs.

The product of this preprocessing regime was a pupil diameter vector for each scanning run which was equal in length to the total number of volumes for that run. This vector was convolved with the informed basis set [canonical hemodynamic response functon (HRF) and its temporal and dispersion derivatives; Friston et al., 1998] to yield three pupil regressors of interest per participant. This step was taken to account for the possibility that the BOLD responses of brainstem nuclei like the LC are not well-modelled solely by the canonical HRF [Wall et al., 2009].

In addition to our use of the averaged measure of pupil diameter outlined above, we also carried out pupil-fMRI analyses that were constructed around stimulus-locked pupillometric indices derived from the task run. These further analyses, which were designed with a view to disentangling phasic versus tonic aspects of the peri-LC BOLD signal [Gilzenrat et al., 2010; Murphy et al., 2011] and probing whether stimulus-evoked BOLD activity (see below) was modulated by single-trial pupil metrics, are reported in greater detail in the Supporting Information.

Physiological Recording

Functional imaging of the LC and adjacent brainstem nuclei is particularly susceptible to multiple kinds of physiological artefact, including quasi-periodic BOLD oscillations introduced by cardiac rhythms and respiration [Harvey et al., 2008]. A tension exists between removing these extraneous sources of variance from the BOLD time-series and yielding a reliable signal from brain regions whose activity correlates with pupil diameter: pupil diameter and heart rate are both affected by changes in sympathetic nervous system activity, and therefore likely share at least some of their total variance. To explore the extent to which removal of heart rate and respiratory signals affected the results of our pupil-fMRI analyses, we implemented retrospective image correction [RETROICOR; Glover et al., 2000]. This method assigns cardiac and respiratory phases to each volume in each participant's fMRI time-series post-hoc, and controls for their effects statistically in the first-level general linear model (GLM). Pre-processing of pulse oximetry and respiration band signals (sampled at 500 Hz) was carried out using the PhLEM toolbox [Verstynen and Deshpande, 2011]. Pulse oximetry time-series were band-pass filtered (0.6–2.0 Hz; Butterworth filter) to isolate cardiac information and respiration band signals were filtered using a Gaussian smoothing kernel with a 400 ms FWHM. Timings of individual peaks, which correspond to maxima in local blood oxygenation in pulse oximetry and peak expansions of the diaphragm in respiration band, were identified using an automated peak detection algorithm (the peakdet function in Matlab; http://www.billauer.co.il/peakdet.html) and the interpeak intervals were transformed into phase-time. This phase information could then be used to estimate the dominant Fourier series of the respective signals and their first harmonics, the sine and cosine components of which were downsampled to the temporal resolution of the EPI sequence (0.5 Hz) and included as regressors of no interest in the GLM. This procedure therefore yielded a total of eight physiological regressors (four cardiac, four respiratory).

Statistical Analysis

First-level single-subject analyses involved the construction of one GLM for each run (rest and task). For a given run, the three pupil diameter regressors for that run constituted the only regressors of interest in the model. Residual effects of head motion were controlled for by using the six head motion parameters estimated during the realignment stage of image preprocessing as regressors of no interest. Two separate control analyses were also devised by constructing variants of this simple GLM. In the first, the eight regressors of no interest derived from the analysis of pulse oxymetry and respiration band data were included in the model in order to correct for physiological noise. In the second, a time-series representing the mean BOLD activity in a mask of area 17 [V1; Amunts et al., 2000] was entered as an additional regressor of no interest in order to exclude the possibility that any observed relationship between pupil diameter and LC could be explained by variations in visual activity. In all of the above, a high-pass filter was employed with a cut-off period of 128 s in order to remove low frequency drifts from the fMRI time-series, in addition to a first-order autoregressive function to account for serial autocorrelations [Smith et al., 2007]. To determine voxels significant at the group level in each model variant, *t*-contrasts for each pupil regressor were incorporated into random-effects analyses (one-way repeated-measures analysis of variance [ANOVA], three levels of pupil/basis-function). All statistical parametric maps (SPMs) were thresholded at $P < 0.001$ uncorrected for display purposes, and all reported results survived peak-level cluster-wise false discovery rate (FDR) correction for multiple comparisons ($P < 0.05$) unless indicated otherwise. A binary image representing overlap between the thresholded SPMs from rest- and task-based pupil analyses was created to determine significant voxels common to both runs.

A series of volume-of-interest (VOI) analyses were also conducted, without physiological correction, to explore LC effects related to stimulus relevance in the oddball task.

The primary VOI was defined by masking a previously published LC atlas [Keren et al., 2009; 2-SD version] with the dorsal pontine cluster identified in the earlier pupil diameter analysis of task runs (see Results section), and the principle eigenvariate of time-courses in all overlapping voxels ($n = 18$) was extracted for each participant [Friston et al., 1996]. Hence, we leveraged our earlier analysis of brain regions that relate to fluctuations in pupil diameter to derive a "functional localizer" for the LC that had greater spatial and functional specificity than the LC atlas considered as a whole [Saxe et al., 2006]. Each VOI time-course was also "adjusted" by an *F*-contrast from the first-level GLMs which included all three pupil diameter regressors—this step effectively partials out any variance in the VOI signal related to regressors of no interest in the first-level GLMs (in this case, related to head movement). Each participant's adjusted VOI time-course then acted as the dependent variable in a multiple regression model in which the onsets for each stimulus type (targets and standards) were modelled separately by convolving event delta functions with the informed basis set (yielding six independent variables). Onsets for miss trials (mean = 2.50, s.d. = 2.35) and false alarms (mean = 1.64, s.d. = 1.78) were not included. This approach yielded beta-weights that indicated the extent to which each stimulus-type drove activity in the LC VOI. These were subjected to a two-way repeated-measures ANOVA (Stimulus-type [Target, Standard] by Basis Function [Canonical, Temporal, Dispersion]) to test for a main effect of stimulus-type. When betas for a given participant were multiplied by their appropriate basis functions, the linear sum within-stimulus-type of the resulting waveforms provided an estimate of the evoked BOLD response to each stimulus-type. The peak of estimated BOLD responses to targets, measured in a 4s window centred on the latency of the grand-average peak, was used in the reported between-subjects correlational analysis (Pearson's *r*; see Results section). Lastly, identical procedures were also employed for two control VOI analyses. In the first, the VOI consisted of all voxels within the LC atlas [Keren et al., 2009] that did not overlap with the pupil-derived dorsal pontine cluster ($n = 25$). In the second, a VOI with an identical voxel count to that used in the primary VOI analysis ($n = 18$) was located to the anterior part of the pontine crossing tract, a white matter tract adjacent to the LC.

Finally, a subset of the above statistical analyses were carried out on both spatially smoothed and unsmoothed fMRI data in order to investigate the effect of spatial smoothing on the observed results.

Localization

Anatomical details of significant clusters were obtained by superimposing the SPMs on the T1 canonical single-subject image from the MNI series, and both the average brainstem T1-TSE image and the binary LC atlas [Keren et al., 2009; 2-SD version] were coregistered to this template for precise LC localization. Results were checked against normalized T1 images of each subject, and the SPM anatomy toolbox [Eickhoff et al., 2005, 2006, 2007] was used to establish cytoarchitectonic probabilities where applicable.

RESULTS

The present study explored the relationship between fluctuations in pupil diameter and BOLD activity in humans, with an emphasis on probing the link between pupil diameter and BOLD signals localized to the LC. We first report the results of a standard fMRI analysis, employing spatial smoothing without correction for physiological noise. Because both spatial smoothing and physiological noise can potentially obscure estimates of LC BOLD activity, we then report separate analyses with retrospective correction for physiological noise [Glover et al., 2000] and without the use of a spatial filter. Finally, we utilize information gleaned from these primary investigations to inform a volume-of-interest analysis of the effect of oddball stimulus-relevance on LC BOLD activity.

Whole-brain Pupil Diameter Analyses

Analysis of spatially smoothed fMRI data without physiological correction revealed that pupil diameter at rest was correlated with BOLD activity in a circumscribed cortico-subcortical network of brain regions (Fig. 2A; Table I). Crucially, a cluster was identified in the dorsal pons that exhibited considerable overlap with a previously published LC atlas [Keren et al., 2009]—40% of total atlas space (17 voxels) fell within the pontine cluster bounds (Fig. 2B). Other brain areas identified at rest included visual cortex, medulla, right insula cortex and bilateral anterior cingulate cortex (ACC). During oddball task performance, pupil diameter correlated with BOLD activity in a more spatially extensive region of dorso-rostral pons extending into midbrain (Fig. 2A,C; Table I). Again, this cluster overlapped with the LC atlas, occupying 42% of atlas space (18 voxels). Pupil diameter also correlated with areas of visual cortex, superior colliculus and bilateral thalamic nuclei during task performance. A cluster localized to ACC was also identified during task, though this did not survive correction for multiple comparisons ($P = 0.08$, FDR-corrected). A binary map showing regions of conjunction between rest- and task-based analyses confirmed that only clusters in dorsal pons (overlapping with 21% of the LC atlas; 9 voxels) and visual cortex were common to both (Fig. 2A). Furthermore, a control analysis in which primary visual cortex activation was regressed out of the BOLD signal revealed that the relationship between pupil diameter and dorsal pontine BOLD activity was almost entirely preserved, suggesting that the observed relationship between pupil diameter and the peri-LC BOLD signal is not mediated by changes in visual activity (Supporting Information Fig. S1 and Table SI).

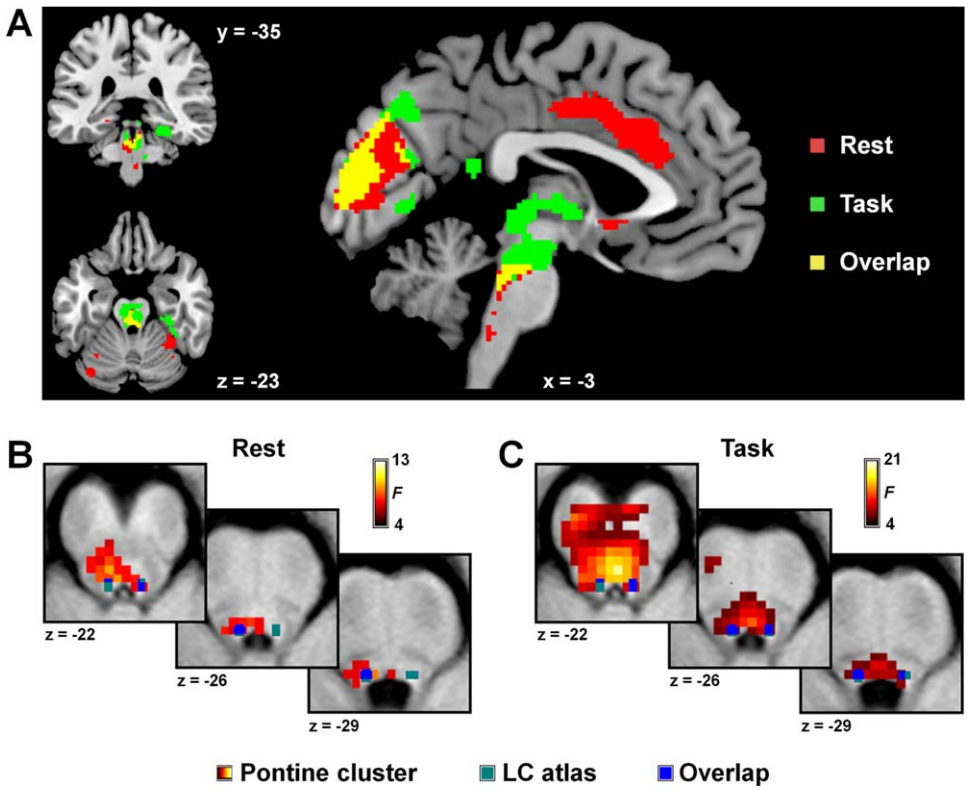

Figure 2.

Relationship between pupil diameter and spatially smoothed BOLD activity. **A**, Whole-brain map showing brain regions whose spatially smoothed BOLD activity covaried with pupil diameter at rest, during oddball task performance, and the overlap between both runs. **B**, Dorsal pontine activation cluster from the rest run (hotter colours indicate higher *F* values) overlayed on the group-mean high-resolution T1 TSE structural image and highlighting overlap with the LC atlas [Keren et al., 2009]. **C**, Dorsal pontine activation cluster from the task run. Same format as B. For A, B, and C, images shown are thresholded at $P < 0.001$ uncorrected, and all regions survived topological FDR correction for multiple comparisons ($P < 0.05$). [Color figure can be viewed in the online issue, which is available at wileyonlinelibrary.com.]

Although the direction of the relationship between pupil diameter and dorsal pontine BOLD activity cannot be ascertained from the above analysis, this information can be obtained by combining the beta coefficients for each level of the informed basis set into an estimated pupil-related BOLD response (see Supporting Information). Application of this procedure revealed that the estimated peri-LC BOLD responses for both rest and task runs were consistently positive, indicating that the relationship between pupil diameter and LC BOLD activity is also positive (Supporting Information Fig. S2).

We also augmented our primary analyses by implementing the RETROICOR method [Glover et al., 2000] to control for effects of potentially extraneous physiological signals (heart rate, respiration) on the observed BOLD time-series. The initial findings were largely recapitulated, pupil diameter being found to correlate with BOLD activity in a restricted cortico-subcortical network at rest (visual cortex, ACC, insula, medulla) and during task performance (visual cortex, thalamus, midbrain; Supporting Information Fig. S3, Table SII). Most importantly, the observed correlation between pupil diameter and peri-LC BOLD activity was again present and its spatial extent was unaffected by the implementation of physiological correction.

The LC has a rostro-caudal extent of 12–17 mm, and a within-plane diameter of just 2.5 mm [Fernandes et al., 2012]. By allowing adjacent voxels to contribute to the estimated signal, application of spatial smoothing to the fMRI data therefore increases the likelihood that the BOLD time-series of voxels localized to the LC are contaminated by noise from surrounding neural tissue. To address this issue, we also explored the relationship between pupil diameter and BOLD activity derived from unsmoothed fMRI data. These analyses yielded a more constrained array of brain regions compared to those identified when spatial smoothing was employed (Fig. 3A; Table II). At rest, only a cluster in visual cortex survived whole-brain

TABLE I. Brain regions covarying with pupil diameter at rest and during oddball task performance

	Cluster	*F* value	*Z* value	Peak co-ordinates	Cytoarchitectonic BA (if available)
Rest					
Right fusiform gyrus	12,005	28.25	6.06	38, −52, −16	n/a
Right inferior occipital gyrus	Same cluster	27.68	6.01	36, −66, −12	hOC4v (V4) (10%)
Left middle occipital gyrus	Same cluster	26.88	5.95	−38, −90, 6	hOC3v (V3v) (30%)
Right superior occipital gyrus	Same cluster	26.52	5.92	26, −78, 34	n/a
Right cuneus	Same cluster	22.79	5.60	14, −86, 22	Area 18 (10%)
Right lingual gyrus	Same cluster	20.51	5.37	22, −56, −6	Area 18 (20%)
Right cerebellum	Same cluster	20.34	5.36	32, −54, −28	Lobule VI (97%)
Bilateral anterior mid-cingulate cortex	925	20.28	5.35	−4, 22, 32	n/a
Bilateral anterior cingulate cortex	Same cluster	13.81	4.54	2, 24, 26	n/a
Right supplementary motor area	Same cluster	11.08	4.09	12, 4, 50	Area 6 (30%)
Bilateral medulla	296	15.75	4.82	4, −36, −46	n/a
Peri-locus coeruleus	Same cluster	12.00	4.25	−4, −32, −30	n/a
Left caudate nucleus	106	14.83	4.69	−14, 8, −12	n/a
Right rolandic operculum	660	14.73	4.68	58, 2, 6	OP4 (30%)
Right insula	Same cluster	11.41	4.15	38, −12, 4	Ig2 (50%)
Right supramarginal gyrus	Same cluster	10.58	4.00	64, −28, 24	IPC (PF) (70%)
Right inferior frontal gyrus	Same cluster	8.47	3.56	50, 8, 4	Area 44 (30%)
Task					
Right superior occipital gyrus	10,006	24.52	5.75	20, −86, 22	n/a
Left superior occipital gyrus	Same cluster	22.94	5.61	−14, −92, 26	Area 17 (10%)
Right middle occipital gyrus	Same cluster	22.57	5.58	44, −74, 8	n/a
Left lingual gyrus	Same cluster	21.19	5.44	−14, −66, −6	hOC4v (V4) (50%), hOC3v (V3) (20%), Area 18 (10%)
Right fusiform gyrus	Same cluster	19.61	5.28	26, −66, −8	hOC4v (V4) (60%), hOC3v (V3) (10%)
Right lingual gyrus	Same cluster	18.84	5.19	12, −74, −6	Area 18 (60%), hOC3v (V3) (60%)
Dorsal pons	2,536	20.39	5.36	−8, −18, −18	n/a
Peri-locus coeruleus	Same cluster	20.13	5.33	2, −30, −22	n/a
Bilateral thalamus	Same cluster	19.11	5.22	6, −6, −2	Th-Prefrontal (85%), Th-Temporal (27%)
Midbrain	Same cluster	16.19	4.88	6, −28, −8	n/a

All regions FDR-corrected for multiple comparisons ($P < 0.05$) in a random effects analysis.
Co-ordinates reported in MNI space.

correction for multiple comparisons. Subsequent small-volume correction using the LC atlas as a mask revealed that BOLD activity in 7% of the total LC atlas (three voxels) was significantly correlated with changes in pupil diameter ($P < 0.05$, FWE-corrected). For the task run, clusters in visual cortex and dorsal pons/midbrain survived whole-brain correction for multiple comparisons. The latter was found to overlap with 16% of the LC atlas (seven voxels). Hence, although the spatial extent of the relationship between pupil diameter and LC BOLD activity was diminished when spatial smoothing was not applied to the fMRI data, a significant relationship between pupil diameter and BOLD activity in a subset of LC voxels persisted.

Why did pupil diameter appear to show a weaker and more spatially limited relationship to LC BOLD activity at rest compared to during task performance? One possible explanation is that task engagement is associated with large dilatory responses in the pupil (Fig. 4A) and evoked responses in the LC (see below). On the other hand, variability in pupil diameter, and indeed the LC BOLD signal, may be too low at rest to achieve a reliable estimate of the strength of the relationship between the two. In support of this possibility, our downsampled tonic pupil diameter time-courses were found to be significantly less variable at rest than during task performance (mean within-subject standard deviation at rest = 0.33 ± 0.12 mm; mean standard deviation during task = 0.41 ± 0.14 mm; paired-samples t test: $t_{13} = 3.60$, $P = 0.003$; Fig. 4B).

Volume-of-interest Stimulus-type Analysis

A cardinal characteristic of single-cell LC activity in non-human primates is a robust phasic response to target stimuli in the oddball task [Aston-Jones et al., 1994; Rajkowski et al., 1994, 2004], though this phenomenon has yet to be demonstrated in humans. In a series of VOI investigations, we sought to leverage the information gleaned from the primary pupillometry-fMRI analyses reported above to explore possible oddball stimulus-type effects on the LC BOLD response. These VOI analyses were carried out on both smoothed and unsmoothed fMRI data, without physiological correction.

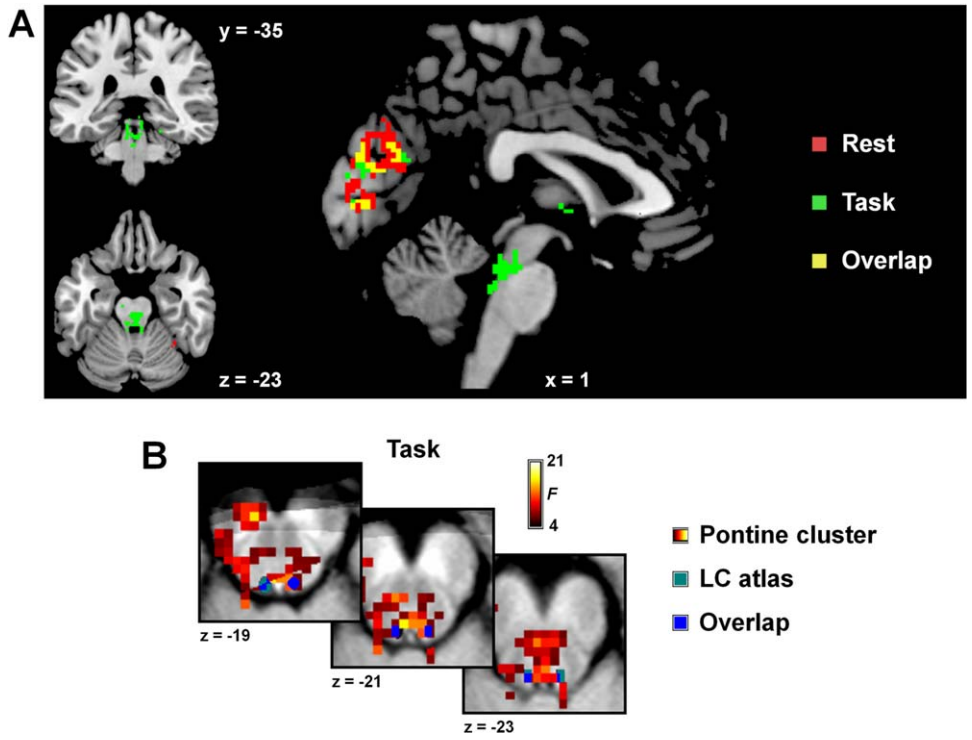

Figure 3.

Relationship between pupil diameter and BOLD activity without spatial smoothing. **A**, Whole-brain map showing brain regions whose unsmoothed BOLD activity covaried with pupil diameter at rest, during oddball task performance, and the overlap between both runs. **B**, Dorsal pontine activation cluster from the task run (hotter colors indicate higher *F* values) overlayed on the group-mean high-resolution T1 TSE structural image and highlighting overlap with the LC atlas [Keren et al., 2009]. At rest, no dorsal pontine voxels survived whole-brain correction for multiple comparisons. For A and B, images shown are thresholded at $P < 0.001$ uncorrected, and all regions survived topological FDR correction for multiple comparisons ($P < 0.05$). [Color figure can be viewed in the online issue, which is available at wileyonlinelibrary.com.]

For the task-run datasets with spatial smoothing, the primary VOI of interest was defined by masking the LC atlas [Keren et al., 2009] with the dorsal pontine cluster identified in the earlier pupil diameter analysis of those datasets. Regression coefficients for each level of the informed basis set within each stimulus-type showed a main effect of stimulus-type ($F_{1,13} = 10.81$, $P = 0.006$), and the corresponding estimated BOLD responses indicated that target stimuli evoked a larger LC response than standard stimuli (Fig. 5A,B). In addition, between-subjects correlations revealed that larger target-evoked BOLD responses within this VOI were robustly associated with faster mean response times (RTs) across subjects ($r = -0.72$, $P = 0.004$; Fig. 5C).

To explore the specificity of these stimulus-evoked BOLD responses to the pupil-localized LC cluster, control VOI analyses were also carried out on (1) all remaining voxels in the LC atlas, and (2) an LC-adjacent region of the pontine crossing white matter tract. Regression coefficients for both control VOIs revealed only nonsignificant trends toward main effects of stimulus-type (remaining LC atlas: $F_{1,13} = 3.69$, $P = 0.08$; white matter control region: $F_{1,13} = 4.66$, $P = 0.05$), driven largely by greater regression coefficients for temporal and dispersion HRF derivatives in the target condition (Fig. 5D,G). Indeed, in contrast to the primary VOI analysis, the estimated waveforms for both VOIs failed to show any significant effects of stimulus-type around the time of the peak BOLD response in each condition (Fig. 5E,H). Furthermore, peak target-evoked BOLD response amplitudes in each control VOI did not correlate with mean RT across subjects (remaining LC atlas: $r = -0.36$, $P = 0.21$; white matter control region: $r = 0.16$, $P = 0.58$; Fig. 5F,I). Finally, a multiple regression model with mean RT as the dependent variable and peak target-evoked BOLD responses from each of the three VOIs as predictor variables yielded a significant regression coefficient only for the primary LC/pupil overlap VOI ($\beta_{\text{overlap}} = -0.90$, $P = 0.011$; $\beta_{\text{remaining}} = 0.27$, $P = 0.38$; $\beta_{\text{WM}} = 0.07$, $P = 0.73$). This indicates that variance unique to the target-evoked BOLD responses in the primary "overlap" VOI was predictive of between-subjects variation in mean RT.

TABLE II. Brain regions covarying with pupil diameter at rest and during oddball task performance, without spatial smoothing of fMRI data

	Cluster	*F* value	*Z* value	Peak co-ordinates	Cytoarchitectonic BA (probability, if available)
Rest					
Right cuneus	3,890	23.60	5.67	10, −86, 22	Area 18 (50%)
Right middle occipital gyrus	Same cluster	19.76	5.29	28, −76, 30	n/a
Left middle occipital gyrus	Same cluster	19.03	5.21	−40, −78, 2	hOC5 (V5) (20%)
Right inferior occipital gyrus	Same cluster	18.50	5.16	38, −78, −2	hOC4v (V4) (10%)
Right fusiform gyrus	Same cluster	15.92	4.84	34, −64, −14	hOC4v (V4) (20%)
Right lingual gyrus	Same cluster	15.73	4.81	8, −68, −2	Area 18 (90%), Area 17 (40%), hOC3v (V3) (20%)
Right superior occipital gyrus	Same cluster	15.64	4.80	24, −78, 28	n/a
Cerebellar vermis	Same cluster	15.16	4.74	6, −72, −10	Lobule VI (37%)
Task					
Right lingual gyrus	3,137	22.37	5.56	12, −72, −8	hOC3v (V3) (60%), Area 18 (50%), Area 17 (10%)
Right fusiform gyrus	Same cluster	21.87	5.51	24, −68, −10	hOC4v (V4) (70%), hOC3v (V3) (30%)
Right middle occipital gyrus	Same cluster	20.60	5.38	44, −76, 6	hOC5 (V5) (20%)
Right superior occipital gyrus	Same cluster	17.45	5.03	24, −84, 26	n/a
Right cuneus	Same cluster	17.30	5.01	12, −92, 24	Area 18 (40%), Area 17 (10%)
Left cuneus	Same cluster	15.81	4.83	−8, −88, 26	Area 18 (20%)
Midbrain	789	22.36	5.56	−6, −32, −12	n/a
Peri-locus coeruleus	Same cluster	17.24	5.01	0, −32, −20	n/a
Dorsal pons	Same cluster	16.58	4.92	−4, −18, −18	n/a
Bilateral thalamus	Same cluster	16.42	4.90	−10, −8, 6	Th-Prefrontal (91%)
Left lingual gyrus	705	18.71	5.18	−12, −66, −6	hOC4v (V4) (40%), Area 18 (30%), hOC3v (V3) (20%)
Left calcarine gyrus	Same cluster	13.42	4.48	−16, −60, 4	Area 17 (40%), Area 18 (10%)
Left fusiform gyrus	Same cluster	13.17	4.45	−24, −74, −10	hOC4v (V4) (50%), hOC3v (V3) (30%), Area 18 (10%)

All regions FDR-corrected for multiple comparisons ($P < 0.05$) in a random effects analysis. Co-ordinates reported in MNI space.

Application of the above VOI analysis procedure to the unsmoothed fMRI data (see Supporting Information) similarly revealed that oddball stimulus-type effects were specific to the region of overlap between the LC atlas and pupil-localized dorsal pontine cluster, and not present in the remainder of the LC atlas (Supporting Information Fig. S5). However, the between-subjects correlation of target-evoked LC activity with mean RT was not observed in the unsmoothed data.

Pupil diameter is phasically modulated by task-relevant stimuli [Beatty, 1982], and we observed such an effect in response to target stimuli in the oddball task (Fig. 4A). It may therefore be possible that our pupil diameter time-course only correlated with BOLD activity in brain areas related to the processing of stimulus relevance, and that this subsequently biased the above VOI analyses of stimulus-type effects. The observation that our continuous, downsampled pupil diameter time-courses from the task runs only correlated significantly with BOLD activity in dorsal pons/midbrain, thalamus and visual cortex speaks against this possibility—if these signals primarily reflected the processing of stimulus relevance, they would be expected to correlate with activity in a broader network of brain regions [e.g., Bledowski et al., 2004; Mantini et al., 2009; see Supporting Information Fig. S5].

Nonetheless, in order to further rule out the possibility that the VOI results were biased in favour of detecting task-relevant BOLD responses, we repeated the analysis using the region of overlap between the LC atlas [Keren et al., 2009] and the dorsal pontine cluster identified at rest as the primary VOI (17 voxels). A control VOI analysis was again carried out using all remaining voxels in the LC atlas ($n = 26$). In keeping with the initial findings, regression coefficients for the primary "overlap" VOI showed a significant main effect of stimulus-type ($F_{1,13} = 8.67$, $P = 0.011$) whereby target stimuli yielded larger coefficients compared to standard stimuli. This effect was reflected in the magnitude of the estimated BOLD responses, with targets evoking a consistently larger response than standards around the time of the waveform peaks (4–6 s post-stimulus). In contrast, regression coefficients for the control VOI again only trended toward a significant main effect of stimulus-type ($F_{1,13} = 4.54$, $P = 0.05$) driven by the temporal and dispersion derivatives, and the estimated waveforms failed to show any stimulus-type effects within the relevant time window. These findings

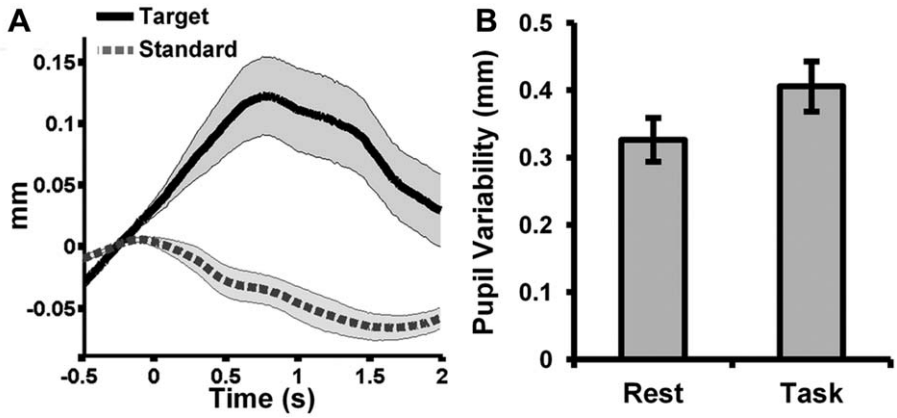

Figure 4.

Characteristics of the pupillometric signals. **A**, Grand-average stimulus-evoked responses in pupil diameter during oddball task performance. The original pupillometric time-course (sampled at 60 Hz) was epoched around stimulus presentation using mean pupil diameter over the 500 ms prestimulus as a baseline. Shaded area represents S.E.M. **B**, Within-subject variability in the continuous, down-sampled pupillometric time-series employed in the fMRI analyses. Error bars indicate S.E.M.; pupil diameter was more variable during the task run compared to the rest run ($P = 0.003$).

mirror our previous VOI results, and suggest that the initial analysis was not biased in favour of detecting stimulus-type effects.

Lastly, we conducted a series of whole-brain voxel-wise analyses that explored both the average effect of oddball stimulus relevance on the BOLD response, and whether this evoked activity was modulated by event-related single-trial measures of pupil dilation (see Supporting Information and Supporting Information Fig. S5). Neither method yielded any significant effects in the vicinity of the LC. Hence, the pupil-informed VOI approach we adopted above appeared to be uniquely sensitive to the effect of oddball stimulus relevance on peri-LC BOLD activity.

DISCUSSION

We report a correlation between continuous pupil diameter and BOLD activity in a circumscribed cortico-subcortical network of brain regions, both at rest and during performance of the two-stimulus oddball task. Importantly, pupil diameter was found to positively correlate with BOLD activity in the rostral LC, as localized via both neuromelanin-sensitive structural imaging [Shibata et al., 2006] and a previously published LC atlas [Keren et al., 2009]. This finding was robust to correction for the effects of cardiac and respiratory activity on the BOLD time-series [Glover et al., 2000], and persisted in a smaller subset of LC voxels when no spatial smoothing was applied to the fMRI data. The comprehensive nature of our analyses, across two different paradigms and with and without the use of physiological correction and spatial smoothing, is unprecedented amongst existing human LC imaging studies [e.g., Kahnt and Tobler, 2013; Krebs et al., 2013; Minzenberg et al., 2008; Raizada and Poldrack, 2007; Schmidt et al., 2009; van Marle et al., 2010], and highlights the stability of the observed relationship between pupil diameter and BOLD activity localized to the LC.

Our results constitute the first functional neuroimaging evidence that lends support to the use of pupil diameter as an indirect index of human LC activity. While several previous studies have combined pupillometry with fMRI [Critchley et al., 2005; Johnstone et al., 2007; Siegle et al., 2003; Sterpenich et al., 2006], a link between BOLD activity localized to the LC and concurrently recorded pupil diameter has not been reported previously. Two features of our analyses may account for the present demonstration of a pupil–LC relationship. First, we devised a continuous, averaged metric of pupil diameter that was not locked to any task-relevant event, and thus stands in contrast to the event-related pupil dilation measure typically employed by previous pupillometry-fMRI studies. While evoked pupil dilation has been proposed to reflect the LC phasic response [Gilzenrat et al., 2010), our continuous measure likely confers several key advantages in the context of attempts to link pupil diameter and peri-LC BOLD activity: it is less susceptible to the effects of trial-by-trial noise; it yields many more observations for analysis, thus improving statistical power; and, it incorporates tonic variation in the pupil diameter time-course, which may exhibit a clearer relationship to the dynamics of the low-frequency BOLD signal. Indeed, we did not observe any significant effects in the vicinity of the LC in a series of supplementary analyses leveraging single-trial, event-locked pupillometric indices, thus highlighting the unique sensitivity of our continuous measure to peri-LC BOLD

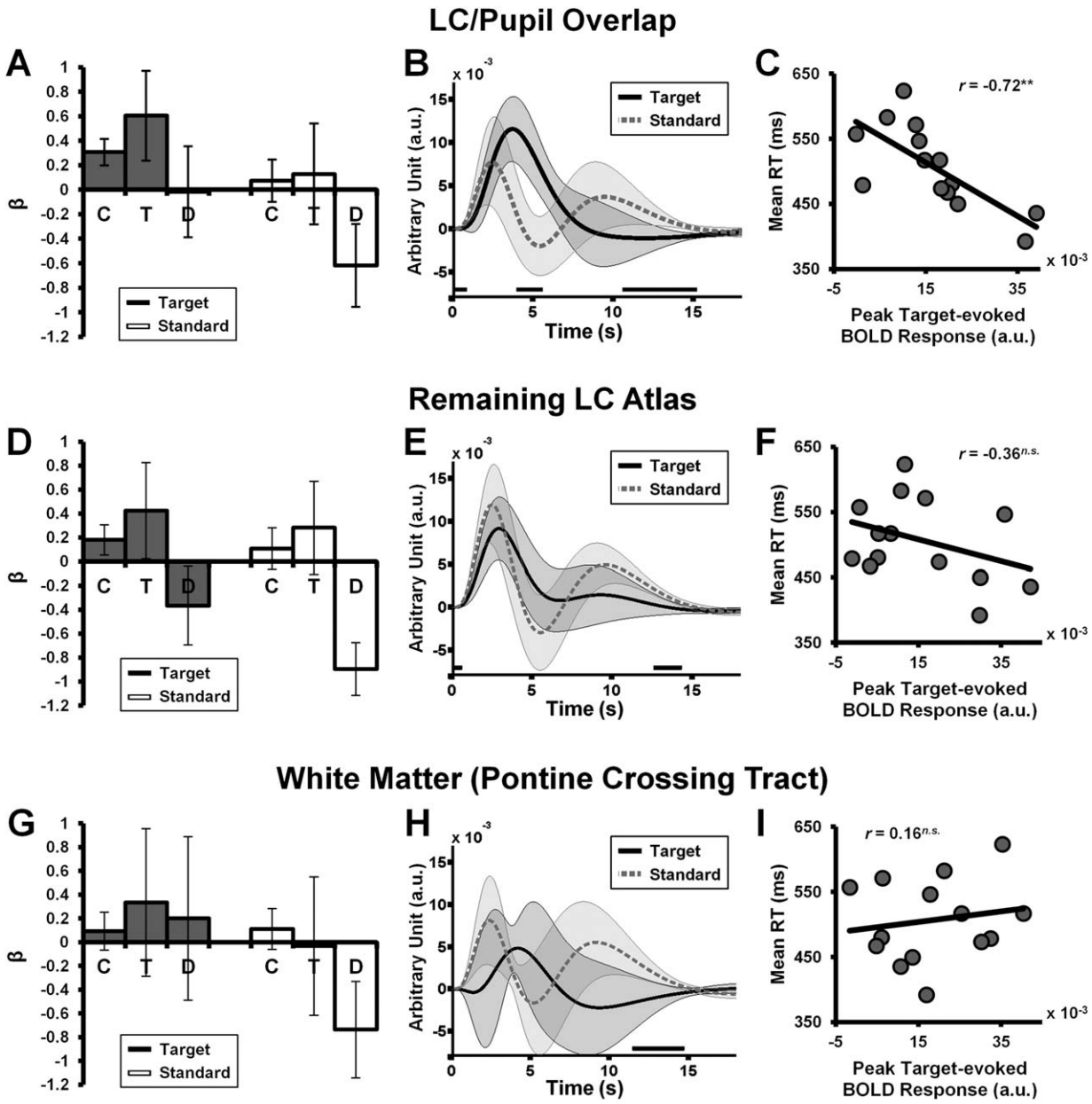

Figure 5.

Volume of interest (VOI) analyses of the effect of oddball stimulus relevance on evoked LC BOLD responses with spatial smoothing. **A**, Parameter estimates for target versus standard stimuli at each level of the informed basis set (C: canonical HRF; T: temporal derivative; D: dispersion derivative), where the VOI was defined by the overlap between the LC atlas and the dorsal pontine cluster identified during the task run ("LC/pupil overlap"). Error bars indicate S.E.M. **B**, Estimated BOLD responses for the LC/pupil overlap VOI, time-locked to stimulus onset. Shaded area represents S.E.M., black lines indicate latencies at which stimulus-type effect was statistically significant ($P < 0.05$, uncorrected). **C**, Between-subjects correlation of response time (RT) with peak target-evoked BOLD response amplitude in the LC/Pupil Overlap VOI. **D–F**, Parameter estimates, estimated BOLD responses and between-subjects correlation for a control VOI defined by all remaining voxels in the LC atlas. Format same as **A–C**, respectively. **G–I**, Parameter estimates, estimated BOLD responses and between-subjects correlation for a second control VOI defined by an LC-adjacent region of the pontine crossing white matter tract. Format same as **A–C**, respectively. $^{**}P < 0.01$; $^{n.s.}P > 0.2$.

effects. One apparent limitation of our continuous pupil measure is that it cannot be used to address the question of whether our observed pupil-LC BOLD coupling is driven by tonic neural activity, phasic activity, or some combination of the two. Unfortunately, supplementary analyses of single-trial pupil metrics that may dissociate both aspects of LC firing [e.g., Gilzenrat et al., 2010] failed to shed light on this question.

A second feature of our approach that likely augmented our sensitivity toward revealing a pupil–LC relationship centered on our use of the informed basis set for modeling BOLD responses [Friston et al., 1998]. The informed basis set affords high flexibility when attempting to model the likely heterogeneous HRFs of different cortical and subcortical brain regions [Handwerker et al., 2004; Wall et al., 2009]. Sole use of the canonical HRF, by contrast, may serve as a poor template for the LC BOLD response, and this possibility has not been taken into account by previous studies combining pupillometry and fMRI. A related advantage conferred by the informed basis set is that it provided a conservative method by which to compensate for any possible lag between the continuous pupil diameter and BOLD time series: By allowing a degree of flexibility in peak latencies of the estimated BOLD responses, convolution with the informed basis set likely diminished the negative impact of signal lag on the strength of the observed relationships. It remains possible, however, that quantifying the effect of signal lag by systematically interrogating the pupil–LC relationship at a variety of temporal offsets may yield even more robust effects than those reported here.

Notably, image correction for cardiac and respiratory activity had little impact on the identified relationship between pupil diameter and the peri-LC BOLD signal. This observation appears to argue in favor of the validity of findings from previous imaging studies that have reported functional effects in the vicinity of the LC but have not attempted to control for physiological artifacts. Nonetheless, subcortical BOLD signals in particular can be strongly affected by sources of physiological noise [Harvey et al., 2008], and it will be important for future LC imaging studies to verify that any observed effects are robust to these.

In addition to the observed relationship with peri-LC BOLD activity, pupil diameter was found to correlate with activity in a relatively sparse network of cortical and subcortical brain regions that included ACC, insula and medulla (rest), thalamus and midbrain including the superior colliculus (task), and visual cortex (both runs). Evidence exists to suggest that several of these identified brain regions are functionally coupled with the LC-NA system. For example, implication of the ACC and insula cortices is in agreement with the strong anatomical [Arnsten and Goldman-Rakic, 1984; Gompf et al., 2010; Jodo et al., 1998] and functional [Minzenberg et al., 2008; Ullsperger et al., 2010] connectivity between these regions and the LC [see also Aston-Jones and Cohen, 2005], whereas thalamus has previously been postulated to act as a relay between the LC and neocortical cognitive control systems [Sturm and Willmes, 2001]. Similarly, the ventral medulla projects profusely to LC [Aston-Jones et al., 1986], and has been hypothesized to mediate the relationship between the LC and pupil diameter [Nieuwenhuis et al., 2010]. Such observations hint at the possibility that cognitively relevant fluctuations in pupil diameter are determined by a constrained cortico-subcortical brain network, of which the LC is an integral part. We also note that, for both rest and task runs, the dorsal pontine activation cluster extended rostral and medial to the LC proper. This finding may be driven by correlations between pupil diameter and the activity of several autonomic nuclei residing in this general area that are known to directly regulate pupillary dynamics [e.g., the Edinger–Westphal nucleus; Szabadi and Bradshaw, 1996].

In a series of volume of interest (VOI) analyses, the region of overlap between the LC atlas [Keren et al., 2009] and the dorsal pontine cluster that correlated with pupil diameter during task performance exhibited a greater evoked response to target stimuli than to standards. This observation constitutes the first demonstration in humans of a cardinal characteristic of animal LC activity: phasic modulation by stimulus-relevance on the oddball task [Aston-Jones et al., 1994; Rajkowski et al., 1994, 2004]. Notably, the same stimulus-type effect was absent when all remaining voxels in the LC atlas were employed in a separate analysis. These findings were replicated both without spatial smoothing, and when the dorsal pontine cluster identified at rest was used to define the respective VOIs. The latter result indicates that the observed LC sensitivity to oddball stimulus relevance persisted even when the VOI was derived from pupil data collected independent of task performance. At the between-subjects level, larger evoked LC BOLD responses to target stimuli were reliably associated with faster mean response times. This finding is consistent with a core tenet of the adaptive gain theory of LC–NA function that phasic LC activity expedites appropriate responses to behaviorally relevant stimuli [Aston-Jones and Cohen, 2005], and again was restricted to the area of overlap between the LC atlas and the task-derived pontine cluster. However, these between-subjects effects were absent when spatial smoothing was not applied to the fMRI data. We note that it was not possible given our task design to disentangle the extent to which target-evoked BOLD responses reflect simple "novelty" processing as opposed to processes related to the behavioral relevance of the stimulus. Future studies could investigate this further by including infrequent nontarget stimuli as part of the oddball task [e.g., Bledowski et al., 2004].

Why did pupil diameter only covary with activity in the rostral LC, and why was the effect of oddball stimulus-type on LC BOLD activity only present in this specific region? One possibility is that our findings could reflect a distinct subpopulation of LC neurons that selectively correlate with pupil diameter and are uniquely sensitive to

stimulus-relevance. While this possibility is intriguing, two sources of evidence derived from animal LC physiology suggest that this may not be the case. First, the ventral medulla, hypothesized to mediate the relationship between LC activity and pupil size [Nieuwenhuis et al., 2010], does not exhibit selectivity in its projections to rat LC along a rostro-caudal axis [van Bockstaele et al., 1998]. Second, the monkey LC phasic response to target oddball stimuli is a stereotyped, LC-wide phenomenon [e.g., Aston-Jones et al., 1994], which does not support an argument for differentiation among LC neurons' phasic sensitivity to stimulus-relevance. In fact, previous LC imaging studies have rarely reported peri-LC clusters that are larger than those reported here [e.g., Kahnt and Tobler, 2013; Krebs et al., 2013; Minzenberg et al., 2008; Raizada and Poldrack, 2007; Schmidt et al., 2009; van Marle et al., 2010], which may reflect the fact that fMRI of brainstem nuclei like the LC is subject to a low signal-to-noise ratio even after extensive image preprocessing [Barry et al., 2013; Harvey et al., 2008]. This in turn suggests another plausible explanation for the spatially constrained nature of our LC functional effects: Pupil diameter correlations and stimulus-type effects were not observed where LC voxel time-series were particularly noisy. Indeed, a control VOI analysis localized to the LC-adjacent pontine crossing white matter tract revealed moderate stimulus-evoked responses in this region, suggesting considerable contamination by noise.

A further consequence of this high degree of noise is that our data likely underestimate the true strength of the pupil–LC relationship, and are therefore unable to provide an accurate assessment of how well pupil diameter actually indexes LC activity. A rigorous analysis of the strength of this relationship using direct cellular recordings in animals will be an important next step in establishing pupil diameter as a robust indirect measure of LC activity. In spite of these issues, however, our VOI analyses do offer encouragement for researchers in search of avenues to overcome the signal-to-noise difficulties inherent in LC functional imaging, by suggesting that pupil diameter might be used to isolate LC voxels with the most reliable signals.

As noted above, some discrepancies existed between the results observed with and without spatial smoothing: When no smoothing was employed, the spatial extent of the LC–pupil relationship was diminished, particularly in the rest condition, and the between-subjects correlation effect was absent. Which, then, is the more appropriate approach? In terms of minimizing the contribution of adjacent brain regions to the observed LC BOLD signal, omitting spatial smoothing is clearly preferable. However, smoothing also offers some distinct advantages, such as improving statistical power by enforcing the parametric assumptions of random field theory, and importantly, diminishing the negative effects of small between-subjects normalization differences on group-level analyses. The latter point is particularly salient for small structures located deep in the brainstem, like the LC, where individual differences in location in standardized space likely persist even after application of sophisticated normalization techniques. We therefore view both smoothed and unsmoothed analyses as complementary, and convergent upon our primary conclusion that pupil diameter correlates with BOLD activity in at least a subset of LC-localized voxels.

Nonetheless, the promise of this observation should be accompanied by several caveats. First, a proportion of LC neurons are intermingled with cells belonging to predominantly cholinergic pontine nuclei such as the laterodorsal tegmental nucleus [Mesulam et al., 1989] which, like the LC, play important roles in the regulation of arousal. Disentangling the unique relationships between pupil diameter and these cell groups is not feasible with fMRI. Second, fMRI images of higher spatial resolution than that employed presently would be more suited to ruling out the possibility that the LC-localized BOLD signal is contaminated by activity from other neighboring brainstem nuclei. Both considerations, coupled with the previously mentioned prospect of individual differences in LC location even after image normalization, highlight the fact that conclusions regarding the extent to which our observed dorsal pontine effects are specific to LC must remain tentative. Future studies should therefore seek to replicate the correlation between pupil diameter and LC activity at finer fMRI image resolution [e.g. Minzenberg et al., 2010] and, more importantly, via single unit recordings in animals.

CONCLUSIONS

The present results provide important support for the increasing use of pupil diameter as a tractable, non-invasive index of LC activity. We have also leveraged the relationship between pupil diameter and LC BOLD activity to provide the first demonstration in humans of phasic LC modulation by stimulus relevance in the classic two-stimulus oddball paradigm. Taken together, these findings highlight the exciting potential for utilizing pupil diameter to achieve a more comprehensive understanding of the role of the LC–NA system in human cognition.

ACKNOWLEDGMENTS

The authors thank Sojo Joseph and for help with MRI data acquisition, Simon Dunne and Timothy Verstynen for assistance with implementation of physiological correction, and Sander Nieuwenhuis for helpful comments on an earlier draft. The MRI protocol was developed by C.M. Kerskens with support from Sojo Joseph at the TCIN. The authors declare no conflicts of interest.

REFERENCES

Amunts K, Malikovic A, Mohlberg H, Schormann T, Zilles K (2000): Brodmann's areas 17 and 18 brought into stereotaxic space-where and how variable? NeuroImage 11:66–84.

Arnsten AF, Goldman-Rakic PS (1984): Selective prefrontal cortical projections to the region of the locus coeruleus and raphe nuclei in the rhesus monkey. Brain Res 306:9–18.

Ashburner J, Friston KJ (2005): Unified segmentation. NeuroImage 26:839–851.

Astafiev SV, Snyder AZ, Shulman GL, Corbetta M (2010): Comment on "Modafinil shifts human locus coeruleus to low-tonic, high-phasic activity during functional MRI" and "Homeostatic sleep pressure and responses to sustained attention in the suprachiasmatic area". Science 328:309.

Aston-Jones G, Cohen JD (2005): An integrative theory of locus coeruleus-norepinephrine function: Adaptive gain and optimal performance. Annu Rev Neurosci 28:403–450.

Aston-Jones G, Ennis M, Pieribone VA, Nickell WT, Shipley MT (1986): The brain nucleus locus coeruleus: Restricted afferent control of a broad efferent network. Science 234:734–737.

Aston-Jones G, Rajkowski J, Kubiak P, Alexinsky T (1994): Locus coeruleus neurons in monkey are selectively activated by attended cues in a vigilance task. J Neurosci 14:4467–4480.

Barry RL, Coaster M, Rogers BP, Newton AT, Moore J, Anderson AW, Zald DH, Gore JC (2013): On the origins of signal variance in FMRI of the human midbrain at high field. PLoS One 8:e62708.

Beatty J (1982): Task-evoked pupillary responses, processing load, and the structure of processing resources. Psychol Bull 91:276–292.

Berman SM, Naliboff BD, Suyenobu B, Labus JS, Stains J, Ohning G, Kilpatrick L, Bueller JA, Ruby K, Jarcho J, Mayer EA (2008): Reduced brainstem inhibition during anticipated pelvic visceral pain correlates with enhanced brain response to the visceral stimulus in women with irritable bowel syndrome. J Neurosci 28:349–359.

Berridge CW, Waterhouse BD (2003): The locus coeruleus-noradrenergic system: Modulation of behavioral state and state-dependent cognitive processes. Brain Res Brain Res Rev 42:33–84.

Bledowski C, Prvulovic D, Hoechstetter K, Scherg M, Wibral M, Goebel R, Linden DE (2004): Localizing P300 generators in visual target and distractor processing: A combined event-related potential and functional magnetic resonance imaging study. J Neurosci 24:9353–9360.

Bouret S, Sara SJ (2004): Reward expectation, orientation of attention and locus coeruleus-medial frontal cortex interplay during learning. Eur J Neurosci 20:791–802.

Bouret S, Sara SJ (2005): Network reset: A simplified overarching theory of locus coeruleus noradrenaline function. Trends Neurosci 28:574–582.

Clayton EC, Rajkowski J, Cohen JD, Aston-Jones G (2004): Phasic activation of monkey locus ceruleus neurons by simple decisions in a forced-choice task. J Neurosci 24:9914–9920.

Critchley HD, Tang J, Glaser D, Butterworth B, Dolan RJ (2005): Anterior cingulate activity during error and autonomic response. NeuroImage 27:885–895.

Dayan P, Yu AJ (2006): Phasic norepinephrine: A neural interrupt signal for unexpected events. Network 17:335–350.

Eickhoff SB, Stephan KE, Mohlberg H, Grefkes C, Fink GR, Amunts K, Zilles K (2005): A new SPM toolbox for combining probabilistic cytoarchitectonic maps and functional imaging data. NeuroImage 5:1325–1335.

Eickhoff SB, Heim S, Zilles K, Amunts K (2006): Testing anatomically specified hypotheses in functional imaging using cytoarchitectonic maps. NeuroImage 15:570–582.

Eickhoff SB, Paus T, Caspers S, Grosbras MH, Evans AC, Zilles K, Amunts K (2007): Assignment of functional activations to probabilistic cytoarchitectonic areas revisited. NeuroImage 36: 511–521.

Einhauser W, Stout J, Koch C, Carter O (2008): Pupil dilation reflects perceptual selection and predicts subsequent stability in perceptual rivalry. Proc Natl Acad Sci USA 105:1704–1709.

Fernandes P, Regala J, Correia F, Goncalves-Ferreira AJ (2012): The human locus coeruleus 3-D stereotactic anatomy. Surg Radiol Anat 34:879–885.

Friston KJ, Poline JB, Holmes AP, Frith CD, Frackowiak RS (1996): A multivariate analysis of PET activation studies. Hum Brain Mapp 4:140–151.

Friston KJ, Fletcher P, Josephs O, Holmes A, Rugg MD, Turner R (1998): Event-related fMRI: Characterizing differential responses. NeuroImage 7:30–40.

Gilzenrat MS, Nieuwenhuis S, Jepma M, Cohen JD (2010): Pupil diameter tracks changes in control state predicted by the adaptive gain theory of locus coeruleus function. Cogn Affect Behav Neurosci 10:252–269.

Glover GH, Li TQ, Ress D (2000): Image-based method for retrospective correction of physiological motion effects in fMRI: RETROICOR. Magn Reson Med 44:162–167.

Gompf HS, Mathai C, Fuller PM, Wood DA, Pedersen NP, Saper CB, Lu J (2010): Locus ceruleus and anterior cingulate cortex sustain wakefulness in a novel environment. J Neurosci 30: 14543–14551.

Handwerker DA, Ollinger JM, D'Esposito M (2004): Variation of BOLD hemodynamic responses across subjects and brain regions and their effects on statistical analyses. NeuroImage 21:1639–1651.

Harvey AK, Pattinson KT, Brooks JC, Mayhew SD, Jenkinson M, Wise RG (2008): Brainstem functional magnetic resonance imaging: Disentangling signal from physiological noise. J Magn Reson Imaging 28:1337–1344.

Hou RH, Freeman C, Langley RW, Szabadi E, Bradshaw CM (2005): Does modafinil activate the locus coeruleus in man? Comparison of modafinil and clonidine on arousal and autonomic functions in human volunteers. Psychopharmacology (Berl) 181:537–549.

Jepma M, Nieuwenhuis S (2011): Pupil diameter predicts changes in the exploration-exploitation trade-off: Evidence for the adaptive gain theory. J Cogn Neurosci 23:1587–1596.

Jodo E, Chiang C, Aston-Jones G (1998): Potent excitatory influence of prefrontal cortex activity on noradrenergic locus coeruleus neurons. Neuroscience 83:63–79.

Johnstone T, van Reekum CM, Urry HL, Kalin NH, Davidson RJ (2007): Failure to regulate: Counterproductive recruitment of top-down prefrontal-subcortical circuitry in major depression. J Neurosci 27:8877–8884.

Kahnt T, Tobler PN (2013): Salience signals in the right temporoparietal junction facilitate value-based decisions. J Neurosci 33: 863–869.

Keren NI, Lozar CT, Harris KC, Morgan PS, Eckert MA (2009): In vivo mapping of the human locus coeruleus. NeuroImage 47: 1261–1267.

Krebs RM, Fias W, Achten E, Boehler CN (2013): Picture novelty attenuates semantic interference and modulates concomitant neural activity in the anterior cingulate cortex and the locus coeruleus. NeuroImage 74C:179–187.

Kuipers JR, Thierry G (2011): N400 amplitude reduction correlates with an increase in pupil size. Front Hum Neurosci 5:61.

Liddell BJ, Brown KJ, Kemp AH, Barton MJ, Das P, Peduto A, Gordon E, Williams LM (2005): A direct brainstem-amygdala-cortical 'alarm' system for subliminal signals of fear. NeuroImage 24:235–243.

Mantini D, Corbetta M, Perrucci MG, Romani GL, Del Gratta C (2009): Large-scale brain networks account for sustained and transient activity during target detection. NeuroImage 44:265–274.

Mesulam MM, Geula C, Bothwell MA, Hersh LB (1989): Human reticular formation: Cholinergic neurons of the pedunculopontine and laterodorsal tegmental nuclei and some cytochemical comparisons to forebrain cholinergic neurons. J Comp Neurol 283:611–633.

Minzenberg MJ, Watrous AJ, Yoon JH, Ursu S, Carter CS (2008): Modafinil shifts human locus coeruleus to low-tonic, high-phasic activity during functional MRI. Science 322:1700–1702.

Minzenberg MJ, Watrous AJ, Yoon JH, La C, Ursu S, Carter CS (2010): Response to comment on "modafinil shifts human locus coeruleus to low-tonic, high-phasic activity during functional MRI." Science 328:309.

Mohanty A, Gitelman DR, Small DM, Mesulam MM (2008): The spatial attention network interacts with limbic and monoaminergic systems to modulate motivation-induced attention shifts. Cereb Cortex 18:2604–2613.

Murphy PR, Robertson IH, Balsters JH, O'Connell RG (2011): Pupillometry and P3 index the locus coeruleus-noradrenergic arousal function in humans. Psychophysiology 48:1532–1543.

Nassar MR, Rumsey KM, Wilson RC, Parikh K, Heasly B, Gold JI (2012): Rational regulation of learning dynamics by pupil-linked arousal systems. Nat Neurosci 15:1040–1046.

Nieuwenhuis S, De Geus EJ, Aston-Jones G (2010): The anatomical and functional relationship between the P3 and autonomic components of the orienting response. Psychophysiology 48: 162–175.

Payzan-LeNestour E, Dunne S, Bossaerts P, O'Doherty JP (2013): The neural representation of unexpected uncertainty during value-based decision making. Neuron 79:191–201.

Preuschoff K, t Hart BM, Einhauser W (2011): Pupil dilation signals surprise: Evidence for noradrenaline's role in decision making. Front Neurosci 5:115.

Raizada RD, Poldrack RA (2007): Challenge-driven attention: Interacting frontal and brainstem systems. Front Hum Neurosci 1:3.

Rajkowski J, Kubiak P, Aston-Jones G (1994): Locus coeruleus activity in monkey: Phasic and tonic changes are associated with altered vigilance. Brain Res Bull 35:607–616.

Rajkowski J, Majczynski H, Clayton E, Aston-Jones G (2004): Activation of monkey locus coeruleus neurons varies with difficulty and performance in a target detection task. J Neurophysiol 92:361–371.

Sara SJ (2009): The locus coeruleus and noradrenergic modulation of cognition. Nat Rev Neurosci 10:211–223.

Sara SJ, Bouret S (2012): Orienting and reorienting: The locus coeruleus meidates cognition through arousal. Neuron 76:130–141.

Saxe R, Brett M, Kanwisher N (2006): Divide and conquer: A defense of functional localizers. NeuroImage 30:1088–1096.

Schilbach L, Eickhoff SB, Cieslik E, Shah NJ, Fink GR, Vogeley K (2011): Eyes on me: An fMRI study of the effects of social gaze on action control. Soc Cogn Affect Neurosci 6:393–403.

Schmidt C, Collette F, Leclercq Y, Sterpenich V, Vandewalle G, Berthomier P, Berthomier C, Phillips C, Tinquely G, Darsaud A, Gais S, Schabus M, Desseilles M, Dang-Vu TT, Salmon E, Balteau E, Dequeldre C, Luxen A, Maguet P, Cajochen C, Peigneux P (2009): Homeostatic sleep pressure and responses to sustained attention in the suprachiasmatic area. Science 324: 516–519.

Shibata E, Sasaki M, Tohyama K, Kanbara Y, Otsuka K, Ehara S, Sakai A (2006): Age-related changes in locus ceruleus on neuromelanin magnetic resonance imaging at 3 Tesla. Magn Reson Med Sci 5:197–200.

Siegle GJ, Steinhauer SR, Stenger VA, Konecky R, Carter CS (2003): Use of concurrent pupil dilation assessment to inform interpretation and analysis of fMRI data. NeuroImage 20:114–124.

Smallwood J, Brown KS, Tipper C, Giesbrecht B, Franklin MS, Mrazek MD, Carlson JM, Schooler JW (2011): Pupillometric evidence for the decoupling of attention from perceptual input during offline thought. PLoS One 6:e18298.

Smallwood J, Brown KS, Baird B, Mrazek MD, Franklin MS, Schooler JW (2012): Insulation for daydreams: A role for tonic norepinephrine in the facilitation of internally guided thought. PLoS One 7:e33706.

Smith AT, Singh KD, Balsters JH (2007): A comment on the severity of the effects of non-white noise in fMRI time-series. NeuroImage 36:282–288.

Sterpenich V, D'Argembeau A, Desseilles M, Balteau E, Albouy G, Vandewalle G, Degueldre C, Luxen A, Collette F, Maquet P (2006): The locus ceruleus is involved in the successful retrieval of emotional memories in humans. J Neurosci 26: 7416–7423.

Sturm W, Willmes K (2001): On the functional neuroanatomy of intrinsic and phasic alertness. NeuroImage 14:S76–S84.

Szabadi E, Bradshaw CM (1996): Autonomic pharmacology of α2-adrenoceptors. J Psychopharm 10:6–18.

Ullsperger M, Harsay HA, Wessel JR, Ridderinkhof KR (2010): Conscious perception of errors and its relation to the anterior insula. Brain Struct Funct 214:629–643.

Usher M, Cohen JD, Servan-Schreiber D, Rajkowski J, Aston-Jones G (1999): The role of locus coeruleus in the regulation of cognitive performance. Science 283:549–554.

van Bockstaele EJ, Colago EE, Aicher S (1998): Light and electron microscopic evidence for topographic and monosynaptic projections from neurons in the ventral medulla to noradrenergic dendrites in the rat locus coeruleus. Brain Res 784:123–138.

van Marle HJ, Hermans EJ, Qin S, Fernandez G (2010): Enhanced resting-state connectivity of amygdala in the immediate aftermath of acute psychological stress. NeuroImage 53:348–354.

Vandewalle G, Schmidt C, Albouy G, Sterpenich V, Darsaud A, Rauchs G, Berken PY, Balteau E, Degueldre C, Luxen A, Maquet P, Dijk DJ (2007): Brain responses to violet, blue, and green monochromatic light exposures in humans: Prominent role of blue light and the brainstem. PLoS One 2:e1247.

Verguts T, Notebaert W (2009): Adaptation by binding: A learning account of cognitive control. Trends Cogn Sci 13:252–257.

Verstynen TD, Deshpande V (2011): Using pulse oximetry to account for high and low frequency physiological artifacts in the BOLD signal. NeuroImage 55:1633–1644.

Wall MB, Walker R, Smith AT (2009): Functional imaging of the human superior colliculus: An optimised approach. NeuroImage 47:1620–1627.

Yu AJ, Dayan P (2005): Uncertainty, neuromodulation, and attention. Neuron 46:681–692.